A relaxation scheme for the approximation of the pressureless Euler equations

Christophe Berthon
MAB UMR 5466 CNRS, Université Bordeaux I, 351 cours de la libération, 33400 Talence, France.
INRIA Futurs, projet ScAlApplix, Domaine de Voluceau-Rocquencourt, B.P. 105, 78153 Le Chesnay Cedex France.

Michael Breuß
MAB UMR 5466 CNRS, Université Bordeaux I, 351 cours de la libération, 33400 Talence, France.

Marc-Olivier Titeux
INRIA Futurs, projet ScAlApplix, Domaine de Voluceau-Rocquencourt, B.P. 105, 78153 Le Chesnay Cedex France.

In the present work, we consider the numerical approximation of pressureless gas dynamics in one and two spatial dimensions. Two particular phenomena are of special interest for us, namely δ-shocks and vacuum states. A relaxation scheme is developed which reliably captures these phenomena. In one space dimension, we prove the validity of several stability criteria, i.e., we show that a maximum principle as well as the TVD property for the discrete velocity component and the validity of discrete entropy inequalities hold. Several numerical tests considering not only the developed first-order scheme but also a classical MUSCL-type second-order extension confirm the reliability and robustness of the relaxation approach. The paper extends previous results on the topic: the stability conditions for relaxation methods for the pressureless case are refined, useful properties for the time stepping procedure are established and two-dimensional numerical results are presented.

Keywords: pressureless gas, relaxation scheme, positivity preserving, entropy inequalities, vacuum

I. INTRODUCTION

In this paper, we are concerned with the numerical approximation of the system of pressureless Euler equations in one and two spatial dimensions. The corresponding systems of equations can be regarded as simplifications of the full Euler equations since the ef-

fects of pressure differences are neglected; however, the reduced systems obtained in this fashion are not strictly hyperbolic anymore. The main features of interest within the pressureless systems are the occurrence of delta-shocks and vacuum states, the latter being a difficult case to deal with numerically.

The numerical method we propose for the approximation of the arising systems of equations is a relaxation method. Besides the detailed construction of the scheme, we show in one space dimension the validity of a maximum principle as well as of the TVD property for the discrete velocity component, and we also obtain discrete entropy inequalities for our scheme. These features are in accordance with the exact solutions of the investigated systems of equations. In addition, we show that the developed relaxation scheme remains positive for positive initial values. Vacuum states are approximated with a very high accuracy while the time step size remains reasonable throughout the simulation of the evolution process. The theoretical investigations are supplemented by numerical tests in one and two spatial dimensions, showing the robustness of the developed relaxation method even in the presence of delta-shocks and vacuum states. By the numerical tests, we also observe that these properties not only hold for the developed first-order scheme; they are also valid for a straightforward MUSCL-type second-order extension of the method.

The system of pressureless Euler equations reads in its two-dimensional form

$$\left\{\begin{array}{rcl} \partial_t \rho + \partial_x (\rho u) + \partial_y (\rho v) & = & 0, \\ \partial_t (\rho u) + \partial_x \left(\rho u^2\right) + \partial_y (\rho uv) & = & 0, \\ \partial_t (\rho v) + \partial_x (\rho uy) + \partial_y \left(\rho v^2\right) & = & 0, \end{array}\right. \tag{1.1}$$

where $t > 0$, $x \in \mathbb{R}$, and $\rho(x, y, t) \geq 0$, $u(x, y, t)$ and $v(x, y, t)$ are in $\mathbb{R}$. Thereby, ρ denotes the density, and u, v denote the velocities of the gas under consideration in x- and y-direction, respectively.

It is a well-recognized fact that gas flow features are formed by two kinds of effects, namely effects of inertia and effects of pressure differences; see for instance [21] for a brief discussion. As already indicated, the system (1.1) and its one-dimensional form can be viewed as simplifications of the corresponding usual system of Euler equations when the effects of pressure differences are neglected. Thus, the study of the pressureless system of Euler equations is of twofold interest: on the one hand, such systems may arise modeling pure transport phenomena. For example, such systems may occur in the context of plasma physics [7] or cosmological models [26]. With respect to the latter field of research, the system (1.1) and its one-dimensional form have been the subject of many mainly theoretically oriented studies within the last years. The reason is that they are the basis for modeling sticky particle dynamics useful for explaining the formation of large scale structures in the universe, see e.g. [6, 8, 11, 15] and the references therein. On the other hand, the splitting of a differential operator into a transport step and a pressure correction step is the basis of some very robust algorithms. As a concrete example we mention here [2] where the 1-D Saint-Venant system for shallow water fluid flow is split into the pure transport system (1.1) in its 1-D form and a pressure correction. However, let us note that the transport equations are regularized in that work after the operator splitting. Similar techniques can be encountered in flux splitting approaches, see e.g. [1, 25].

The numerical difficulties when dealing with the occurrence of vacuum states and densities close to vacuum are recognized within the literature, see for instance [11, 14] for discussions. Especially, in the context of pressureless gas dynamics, Bouchut, Jin and

Li [9] have introduced a kinetic scheme as a means for approximation. Also, in [9] a special procedure is introduced in order to obtain a reasonable time step size even in the presence of very low densities. In the context of relaxation schemes, Bouchut proposed to use the same idea, leading to an additional transport equation within the relaxation system considered [4]. Concerning the usual setting of relaxation approximations, see e.g. [3, 4, 13, 18], this is a notable feature since an additional equation should be treated in the same fashion as the remaining relaxation system. In the present work, we establish that no such correction is needed when using the relaxation method if the initial density is positive, an assumption also needed by Bouchut et al. [9] in order to apply the correction proposed there.

For the numerical tests, we not only consider the first-order relaxation scheme investigated before; we also propose a MUSCL-type second-order extension of this scheme. For the one-dimensional test cases, we compare both relaxation schemes with the first- and second-order kinetic schemes given in [9], respectively. The results are qualitatively identical; let us note in this context that kinetic schemes and relaxation methods are connected so that a similar behavior of numerical solutions is no surprise. However, we obtain a much better approximation of the vacuum state which may be an advantage for some applications. In addition, we present results of two-dimensional computations whereby our test case is deduced from the cosmological background mentioned above; thereby, as usual when focusing on the transport stage, we neglect gravitational influences. The numerical results for this test case reveal similar patterns as discussed in [23] while the vacuum is reliably approximated, indicating that the relaxation scheme developed here may be a useful tool for the simulation of cosmological phenomena as well as for performing transport steps within other algorithms.

The paper is organized as follows. In the second section, we discuss the relaxation model for the 1-D case. After that, the first-order relaxation solver is developed, incorporating the detailed description of the actual scheme, its stability properties and a discussion of the vacuum case. The fourth section is devoted to the presentation of numerical experiments.

II. THE RELAXATION MODEL

After the works of Chen, Levermore and Liu [10], Liu [20], Suliciu [22] and more recently of Coquel and Perthame [13] (see also [3, 12] for several applications), the relaxation method can be viewed as a well-established tool to approximate the solutions of the compressible Euler equations of gas dynamics. The main feature of relaxation solvers is to use a relaxation system for which the solution of the Riemann problem is easy to compute.

Of particular interest in the context of this paper is the Suliciu relaxation system described in [13, 22] as well as by Bouchut [4, 5] which is devoted to the resolution of the isentropic Euler equations of gas dynamics or some derivate system, see [3].

In the style of the Suliciu approach, we derive a relaxation model in the framework of the one-dimensional pressureless gas dynamics, i.e., for the system of equations

$$\begin{cases} \partial_t \rho + \partial_x \rho u = 0, & x \in \mathbb{R},\, t > 0, \\ \partial_t \rho u + \partial_x \rho u^2 = 0. \end{cases} \tag{2.1}$$

We introduce a new state variable Π, and we propose as a relaxation model the system

$$\begin{cases} \partial_t \rho^\lambda + \partial_x \rho^\lambda u^\lambda = 0, \qquad x \in \mathbb{R},\, t > 0, \\ \partial_t \rho^\lambda u^\lambda + \partial_x (\rho^\lambda (u^\lambda)^2 + \Pi^\lambda) = 0, \\ \partial_t \rho^\lambda \Pi^\lambda + \partial_x (\rho^\lambda \Pi^\lambda u^\lambda + a^2 u^\lambda) = -\lambda \rho^\lambda \Pi^\lambda, \end{cases} \tag{2.2}$$

with the inverse relaxation rate λ, see for instance Jin and Xin [18], and where the positive relaxation parameter a is detailed later on. For simplicity, the superscript λ indicating the dependence of an actual solution of (2.2) on the relaxation rate will be omitted when appropriate in the sequel. Employing the simplified notations, the system (2.2) can be rewritten in the abstract form

$$\partial_t \mathbf{v} + \partial_x \mathcal{G}_a(\mathbf{v}) = \lambda \mathcal{R}(\mathbf{v}), \tag{2.3}$$

whereby the associated admissible state space $\mathcal{V}$ reads

$$\mathcal{V} = \left\{ \mathbf{v} = (\rho,\, \rho u,\, \rho\Pi)^T \in \mathbb{R}^3;\, \rho > 0,\, u \in \mathbb{R},\, \Pi \in \mathbb{R} \right\}.$$

In fact, the considered model exactly coincides with the relaxation model proposed in [3, 4] in the framework of the isentropic gas dynamic system but for an equilibrium state defined by a zero pressure. This specific property of the system involves several difficulties. As indicated within the introduction, the main one turns out to be the vacuum case.

In [4], a specific relaxation model is proposed to approximate solutions with vacuum. In the following, we establish that the scheme obtained from the relaxation model (2.2) is relevant, in a sense to be made precise, to approximate vacuum solutions of (2.1). This result will be obtained in addition to stability properties like discrete entropy inequalities, a maximum principle on the velocity u and the TVD property on u.

Now, let us state the basic properties of the relaxation system (2.2).

Lemma 2.1. *Assume that $a > 0$. For any $\mathbf{v} \in \mathcal{V}$, the first-order system extracted from (2.2), i.e.,*

$$\begin{cases} \partial_t \rho^\lambda + \partial_x \rho^\lambda u^\lambda = 0, \\ \partial_t \rho^\lambda u^\lambda + \partial_x (\rho^\lambda (u^\lambda)^2 + \Pi^\lambda) = 0, \\ \partial_t \rho^\lambda \Pi^\lambda + \partial_x (\rho^\lambda \Pi^\lambda u^\lambda + a^2 u^\lambda) = 0, \end{cases} \tag{2.4}$$

admits the eigenvalues u and $u \pm a/\rho$ with three linearly independent eigenvectors. As a consequence, the first-order system extracted from (2.2) is hyperbolic. Moreover, each field is associated with a linearly degenerate field.

Proof. Easy calculations ensure that the vectors $\mathbf{r}_i(\mathbf{v})$, $1 \le i \le 3$, given by

$$\mathbf{r}_1(\mathbf{v}) = (\rho,\, -a/\rho,\, a^2/\rho)^T, \quad \mathbf{r}_2(\mathbf{v}) = (1,\, 0,\, 0)^T, \quad \mathbf{r}_3(\mathbf{v}) = (\rho,\, a/\rho,\, a^2/\rho)^T$$

are, respectively, the right eigenvectors for the eigenvalues $\mu_1(\mathbf{v}) = u - a/\rho$, $\mu_2(\mathbf{v}) = u$ and $\mu_3(\mathbf{v}) = u + a/\rho$. As long as a is nonzero, these vectors are linearly independent and the system (2.4) is thus hyperbolic. In addition, it is easy to see that

$$\nabla \mu_i(\mathbf{v}) \cdot \mathbf{r}_i(\mathbf{v}) = 0$$

holds for all $\mathbf{v} \in \mathcal{V}$ with $1 \le i \le 3$. The proof is thus complete. ∎

Let us point out that the linear degeneracy of each of the characteristic fields of (2.4) is actually a desirable property since it ensures that the Riemann problem associated with (2.2) can be solved in a straightforward fashion for $\lambda = 0$.

For the relaxation parameter λ tending to infinity, we formally recover from (2.2) the initial system (2.1). Indeed, in this limit refered to as the *equilibrium limit*, we have $\Pi^\lambda = 0$ implying the conservation of the momentum ρu in (2.1).

Let us note from now on that, after the work of Liu [20] and Chen, Levermore and Liu [10], both systems (2.1) and (2.2) must satisfy compatibility conditions to prevent instabilities in the regime of infinite λ. This so-called sub-characteristic Whitham condition [24] reads as follows:

$$a > 0. \tag{2.5}$$

We will see that this condition enters the analysis of the numerical scheme.

III. THE RELAXATION SOLVER

We propose to derive from the relaxation system (2.2) an approximate Riemann solver for the equilibrium system (2.1). The numerical procedure we develop is standard within the framework of relaxation schemes, see e.g. Jin and Xin [18] or LeVeque [19]. Since the Riemann problem associated with the system (2.2) is trivially solved (each field is linearly degenerate), the relaxation scheme we propose in the present work is based on a Godunov method for (2.2). However, in the framework of the pressureless gas dynamic system (2.1), the scheme must satisfy additional stability properties (i.e., a maximum principle and the TVD property with respect to the velocity) in order to be able to capture vacuum solutions.

For the sake of completeness, we briefly recall the numerical relaxation procedure to approximate weak solutions of (2.1).

Let an approximation of the equilibrium solution at time t^n be given as

$$\mathbf{u}^n(x) = (\rho^n,\, (\rho u)^n)^T(x).$$

In order to evolve this initial data in time, we propose to solve the relaxation model (2.2) in the limit of $\lambda \to \infty$. To approximate the solution at time level $t^{n+1} = t^n + \Delta t$, a splitting technique is adopted. In a first step, we solve (2.4), i.e., the first-order system extracted from (2.2). The second step is devoted to the relaxation source terms in the limit of $\lambda \to \infty$.

First step: Evolution in time. For $t^n \le t < t^n + \Delta t$, the Cauchy problem for the relaxation system (2.2) is solved by setting λ to zero. Thereby, the initial data $\mathbf{v}^n$ are prescribed by the equilibrium approximation $\mathbf{u}^n$:

$$\mathbf{v}^n(x) = (\rho^n,\, (\rho u)^n,\, \rho^n \Pi^{\lambda,n})^T(x). \tag{3.1}$$

Let us emphasize that, for $\lambda = 0$, we have $\Pi^{\lambda,n} = \Pi^{0,n} = 0$ since $\mathbf{v}^n$ is given at the equilibrium. At the end of this first step, the solution is given by $\mathbf{v}(x,t)$.

Second step: Relaxation. The second step of the splitting takes the relaxation source terms into account by solving the ODE system

$$\begin{cases} \partial_t \rho = 0, \\ \partial_t \rho u = 0, \\ \partial_t \rho \Pi = -\lambda \rho \Pi, \end{cases}$$

whereby the solution $\mathbf{v}(x, t^n + \Delta t)$ of the *first step* serves as initial data. In the limit of the relaxation parameter λ tending to ∞, the solution is given by

$$\rho^{n+1}(x) = \rho(x, t^n + \Delta t),\ (\rho u)^{n+1}(x) = (\rho u)(x, t^n + \Delta t) \quad \text{and} \quad \Pi^{\lambda,n+1} = \Pi^{\infty,n+1} = 0.$$

Then we can continue the algorithm since the initial states to be prescribed at the *first step* are now defined.

Thus, the numerical procedure can be summarised as follows: for a given sequence $\mathbf{u}_{i\in\mathbb{Z}}^n$ we define the sequence $\mathbf{v}_{i\in\mathbb{Z}}^n$ setting $\Pi_i^{\lambda,n} = 0$, and $\mathbf{v}_i^n$ is evolved in time by solving (2.4).

In the sequel, we adopt a Godunov scheme to perform this time evolution to obtain $\mathbf{v}_i^{n+1}$ and then $\mathbf{u}_i^{n+1}$.

A. The relaxation scheme

Now, we give the description of the numerical method. Therefore, we consider a structured mesh in space and time, defined by the cells $I_i = [x_{i-\frac{1}{2}}, x_{i+\frac{1}{2}})$ and the time intervals $[t^n, t^{n+1})$:

$$t^{n+1} = t^n + \Delta t \quad \text{and} \quad x_{i+\frac{1}{2}} = \left(i + \frac{1}{2}\right)\Delta x \quad \text{with} \quad i \in \mathbb{Z},\ n \in \mathbb{N},$$

where Δt is the time increment and Δx the spatial cell width. The time increment Δt may vary from an iteration to another according to the CFL stability condition (3.2).

As usual, we consider piecewise constant approximate equilibrium solutions $\mathbf{u}^h(x,t) : \mathbb{R}\times\mathbb{R}_+ \to \Omega$ defined by

$$\mathbf{u}^h(x,t) = \mathbf{u}_i^n = (\rho_i^n,\ (\rho u)_i^n)^T, \quad (x,t) \in I_i \times [t^n, t^{n+1}).$$

At the initial time $t = 0$, we set

$$\mathbf{u}_i^0 = \frac{1}{\Delta x}\int_{x_{i-\frac{1}{2}}}^{x_{i+\frac{1}{2}}} (\rho^0,\ (\rho u)^0)^T(x)\,dx.$$

In order to evolve in time the equilibrium approximate solution, we introduce $\mathbf{v}^h(x,t) : \mathbb{R}\times\mathbb{R}_+ \to \mathcal{V}$ which is piecewise constant at every time level t^k, $k \in \mathbb{N}$. With $\tilde{t} \in (0, \Delta t)$, $\mathbf{v}^h(x, t^n + \tilde{t})$ is the weak solution of the Cauchy problem for (2.2) with $\lambda = 0$ using the following initial data:

$$\mathbf{v}^h(x, t^n) = \mathbf{v}_i^n = (\rho_i^n,\ (\rho u)_i^n,\ \rho_i^n \Pi_i^{\lambda,n} = 0)^T.$$

Under the CFL-like condition

$$\frac{\Delta t}{\Delta x}\max|\mu_i(\mathbf{v}^h)| \le \frac{1}{2}, \tag{3.2}$$

the solution $\mathbf{v}^h$ at $t^n + \Delta t$ is composed of the juxtaposition of the solutions of non-interacting Riemann problems arising at the cell interfaces $x_{i+\frac{1}{2}}$, $i \in \mathbb{Z}$.

The projection of $\mathbf{v}^h(x, t^n + \Delta t)$ on piecewise constant functions undertaken as the next step in the construction of our algorithm yields

$$\mathbf{v}_i^{n+1,-} = \frac{1}{\Delta x}\int_{x_{i-\frac{1}{2}}}^{x_{i+\frac{1}{2}}} \mathbf{v}^h(x, t^{n+1})\,dx.$$

In the present work, we propose to consider a local definition of the parameter a which will be assumed to be constant over each cell (x_i, x_{i+1}), but may vary from one cell to another. We set $a_{i+\frac{1}{2}}$ to characterize this parameter on the cell (x_i, x_{i+1}). Employing the formalism introduced by Harten, Lax and van Leer [17] which is particularly well-suited for a local definition of the parameter a at each interface $x_{i+\frac{1}{2}}$, $i \in \mathbb{Z}$, see [3, 13], we rewrite the latter equation as

$$\mathbf{v}_i^{n+1,-} = \frac{1}{2}\left(\bar{\mathbf{v}}_R(\mathbf{v}_{i-1}^n, \mathbf{v}_i^n; a_{i-\frac{1}{2}}) + \bar{\mathbf{v}}_L(\mathbf{v}_i^n, \mathbf{v}_{i+1}^n; a_{i+\frac{1}{2}})\right), \tag{3.3}$$

where

$$\begin{aligned}\bar{\mathbf{v}}_L(\mathbf{v}_L, \mathbf{v}_R; a) &= \frac{2\Delta t}{\Delta x}\int_{-\frac{\Delta x}{2\Delta t}}^{0} w_a(\xi; \mathbf{v}_L, \mathbf{v}_R)\, d\xi, \\ &= \mathbf{v}_L - \frac{2\Delta t}{\Delta x}\left(\mathcal{G}_a(w_a(0^+; \mathbf{v}_L, \mathbf{v}_R)) - \mathcal{G}_a(\mathbf{v}_L)\right)\end{aligned} \tag{3.4}$$

and

$$\begin{aligned}\bar{\mathbf{v}}_R(\mathbf{v}_L, \mathbf{v}_R; a) &= \frac{2\Delta t}{\Delta x}\int_{0}^{\frac{\Delta x}{2\Delta t}} w_a(\xi; \mathbf{v}_L, \mathbf{v}_R)\, d\xi, \\ &= \mathbf{v}_R - \frac{2\Delta t}{\Delta x}\left(\mathcal{G}_a(\mathbf{v}_R) - \mathcal{G}_a(w_a(0^+; \mathbf{v}_L, \mathbf{v}_R))\right).\end{aligned} \tag{3.5}$$

For a constant fixed parameter a, the function $\mathcal{G}_a$ refers to the exact flux function of the relaxation system (2.2) while $w_a(.; \mathbf{v}_L, \mathbf{v}_R)$ denotes the solution of the Riemann problem for (2.2) with the initial data $v_0(x) = \mathbf{v}_L$ if $x < 0$ and $\mathbf{v}_R$ otherwise.

As long as $\mathbf{v}_L = \mathbf{v}(\mathbf{u}_L)$ and $\mathbf{v}_R = \mathbf{v}(\mathbf{u}_R)$ are defined according to the equilibrium (*i.e.*, $\Pi_L = \Pi_R = 0$),

$$\mathcal{G}_a^{\rho}(\mathbf{v}_{L,R}) = \rho_{L,R} u_{L,R} \quad \text{and} \quad \mathcal{G}_a^{\rho u}(\mathbf{v}_{L,R}) = \rho_{L,R}(u_{L,R})^2$$

hold independently from the choice of the parameter a.

Finally, we evolve the equilibrium solution in time, and so we set

$$\mathbf{u}_i^{n+1} := \left(\rho_i^{n+1} = \rho_i^{n+1,-},\, (\rho u)_i^{n+1} = (\rho u)_i^{n+1,-}\right)^T \tag{3.6}$$

in each cell I_i.

The scheme can then be summarised as follows:

$$\mathbf{u}_i^{n+1} = \mathbf{u}_i^n - \frac{\Delta t}{\Delta x}\left(\mathcal{F}_{i+\frac{1}{2}}^n - \mathcal{F}_{i-\frac{1}{2}}^n\right), \tag{3.7}$$

where

$$\begin{aligned}\mathcal{F}_{i+\frac{1}{2}}^n &= \mathcal{F}(\mathbf{u}_i^n, \mathbf{u}_{i+1}^n), \\ &= \begin{pmatrix} \mathcal{G}^{\rho}_{a_{i+\frac{1}{2}}}\left(w_{a_{i+\frac{1}{2}}}(0^+; \mathbf{v}(\mathbf{u}_i^n), \mathbf{v}(\mathbf{u}_{i+1}^n))\right) \\ \mathcal{G}^{\rho u}_{a_{i+\frac{1}{2}}}\left(w_{a_{i+\frac{1}{2}}}(0^+; \mathbf{v}(\mathbf{u}_i^n), \mathbf{v}(\mathbf{u}_{i+1}^n))\right) \end{pmatrix}.\end{aligned} \tag{3.8}$$

The numerical procedure we have just described is thus written in the style of a finite volume method. Let us emphasize that the value $a_{i+\frac{1}{2}}$ may vary from one cell interface to another because of the influence of the CFL condition (3.2).

To conclude the presentation of the relaxation scheme, we give the exact solution of the Riemann problem for the system (2.2) with $\lambda = 0$ which we need for the Godunov solver.

We recall that all the fields are linearly degenerate. The solution is thus composed of four constant states separated by three contact discontinuities, see Godlewski and Raviart [16]. For the initial data $\mathbf{v}_0(x) = \mathbf{v}_L$ if $x < 0$ and $\mathbf{v}_R$ otherwise, with $\mathbf{v}_L$ and $\mathbf{v}_R$ in $\mathcal{V}$, the Riemann solution always reads

$$\mathbf{v}(x,t) = \begin{cases} \mathbf{v}_L & \text{if } \frac{x}{t} < \mu_1, \\ \mathbf{v}_j & \text{if } \mu_j < \frac{x}{t} < \mu_{j+1},\ j = 1,2, \\ \mathbf{v}_R & \text{if } \frac{x}{t} > \mu_3, \end{cases}$$

where the eigenvalues μ_j (μ_j is the speed of propagation of the jth-contact discontinuity) are assumed to be increasingly ordered.

Lemma 3.1. *Let us set*

$$\begin{aligned} &u^\star = \frac{u_L + u_R}{2},\ \Pi^\star = \frac{\Pi_L + \Pi_R}{2} + \frac{a}{2}(u_L - u_R), \\ &\frac{1}{\rho_L^\star} = \frac{1}{\rho_L} + \frac{u_R - u_L}{2a} + \frac{\Pi_L - \Pi_R}{2a^2},\ \frac{1}{\rho_R^\star} = \frac{1}{\rho_R} + \frac{u_R - u_L}{2a} - \frac{\Pi_L - \Pi_R}{2a^2}. \end{aligned} \tag{3.9}$$

Assume that a is large enough to ensure $\rho_L^\star$ and $\rho_R^\star$ to be positive. Then, the eigenvalues are increasingly re-ordered: $\mu_1(\mathbf{v}_L) < \mu_2(\mathbf{v}_1) < \mu_3(\mathbf{v}_2)$. The intermediate states are given by

$$\mathbf{v}_1 = \begin{pmatrix} \rho_L^\star \\ \rho_L^\star u^\star \\ \rho_L^\star \Pi^\star \end{pmatrix}, \quad \mathbf{v}_2 = \begin{pmatrix} \rho_R^\star \\ \rho_R^\star u^\star \\ \rho_R^\star \Pi^\star \end{pmatrix}. \tag{3.10}$$

Let us note that the requirement for positivity of the intermediate densities $\rho_L^\star$ and $\rho_R^\star$ (a large enough) has nothing to do with the stability condition (2.5). As a consequence, this requirement imposes an additional restriction on the parameter a.

Before we prove Lemma 3.1, let us state without a proof a special case of the above result where $\mathbf{v}_L = \mathbf{v}(\mathbf{u}_L)$ and $\mathbf{v}_R = \mathbf{v}(\mathbf{u}_R)$ correspond to the equilibrium.

Proposition 3.2. *Let us assume that $\Pi_L = 0$ and $\Pi_R = 0$. Let us set*

$$\begin{aligned} &u^\star = \frac{u_L + u_R}{2},\ \Pi^\star = \frac{a}{2}(u_L - u_R), \\ &\frac{1}{\rho_L^\star} = \frac{1}{\rho_L} + \frac{u_R - u_L}{2a},\ \frac{1}{\rho_R^\star} = \frac{1}{\rho_R} + \frac{u_R - u_L}{2a}. \end{aligned} \tag{3.11}$$

Assume that

$$a > \max\left(0,\ \rho_L \frac{u_L - u_R}{2},\ \rho_R \frac{u_L - u_R}{2}\right). \tag{3.12}$$

Then, the intermediate states are given by (3.10)-(3.11).

Proof of the Lemma 3.1. The Riemann solution is uniquely composed of contact discontinuities. We recall that across the jth-contact discontinuity, the Riemann invariants associated with the jth-eigenvector are continuous. These Riemann invariants,

denoted φ_j, are defined by $\nabla\varphi_j \cdot \mathbf{r}_j = 0$ where $\mathbf{r}_j$ is the jth right eigenvector. After a straightforward computation, we obtain the following Riemann invariants (two invariants per field):

$$\begin{array}{ll} \varphi_1^1 = u - \dfrac{a}{\rho}, & \varphi_1^2 = \Pi + au, \\ \varphi_2^1 = u, & \varphi_3^2 = \Pi, \\ \varphi_3^1 = u + \dfrac{a}{\rho}, & \varphi_3^2 = \Pi - au. \end{array}$$

Now, exploiting the continuity of these invariants across the associated contact discontinuity, we obtain the following system of equations:

$$\begin{cases} u_L - \frac{a}{\rho_L} = u_1 - \frac{a}{\rho_1}, \\ \Pi_L + au_L = \Pi_1 + au_1, \end{cases} \quad \text{at the first contact wave,}$$

$$\begin{cases} u_1 = u_2, \\ \Pi_1 = \Pi_2, \end{cases} \quad \text{at the second contact wave,}$$

$$\begin{cases} u_2 + \frac{a}{\rho_2} = u_R - \frac{a}{\rho_R}, \\ \Pi_2 + au_2 = \Pi_R + au_R, \end{cases} \quad \text{at the third contact wave.}$$

The unique solution of this system is given by

$$\rho_1 = \rho_L^\star,\ \rho_2 = \rho_R^\star,\ u_1 = u_2 = u^\star,\ \Pi_1 = \Pi_2 = \Pi^\star,$$

where $\rho_L^\star$, $\rho_R^\star$, $u^\star$ and $\Pi^\star$ are defined by (3.9). ∎

B. The stability properties

Now, we turn to consider the stability properties for one space dimension; namely the discrete maximum principle concerning the velocity, the discrete entropy inequalities and also the discrete TVD property of the velocity. All these properties are satisfied by the exact solutions of (2.1) and should be satisfied also at the discrete level.

In order to establish these properties, we rewrite the scheme (3.7)-(3.8) as follows:

$$\rho_i^{n+1} = \frac{1}{2}\Big(\bar\rho_R(\mathbf{v}_{i-1}^n, \mathbf{v}_i^n; a_{i-\frac12}) + \bar\rho_L(\mathbf{v}_i^n, \mathbf{v}_{i+1}^n; a_{i+\frac12})\Big), \tag{3.13}$$

$$(\rho u)_i^{n+1} = \frac{1}{2}\Big((\bar{\rho u})_R(\mathbf{v}_{i-1}^n, \mathbf{v}_i^n; a_{i-\frac12}) + (\bar{\rho u})_L(\mathbf{v}_i^n, \mathbf{v}_{i+1}^n; a_{i+\frac12})\Big), \tag{3.14}$$

with the notations introduced in (3.4) and (3.5). In the sequel, $\mathbf{v}^n$ is always assumed to be in accordance with the equilibrium state, *i.e.*, $\mathbf{v}^n = \mathbf{v}(\mathbf{u}^n)$.

The first result of this section is as follows.

Theorem 3.3. *Assume that the parameter a satisfies the condition (3.12). Assume also the validity of the CFL like condition (3.2). Then the following maximum principle concerning the velocity is satisfied:*

$$u_i^{n+1} \le \max(u_{i-1}^n,\, u_i^n,\, u_{i+1}^n).$$

In addition, for all real convex functions S, we have the following discrete entropy inequality:

$$\frac{S(u_i^{n+1}) - S(u_i^n)}{\Delta t} + \frac{U(u_i^n, u_{i+1}^n) - U(u_{i-1}^n, u_i^n)}{\Delta x} \le 0,$$

where $U(.,.)$ is the numerical entropy flux function.

Proof. Using the reformulation (3.13)-(3.14) of the relaxation scheme, we propose to rewrite the velocity-update formula as follows:

$$u_i^{n+1} = \frac{\bar\rho_R^{i-\frac12}}{\bar\rho_R^{i-\frac12}+\bar\rho_L^{i+\frac12}} \int_0^{\frac{2\Delta t}{\Delta x}} u\big(w_{a_{i-\frac12}}(\xi;\mathbf{v}_{i-1}^n,\mathbf{v}_i^n)\big)\, dm^+_{i-\frac12} + \frac{\bar\rho_L^{i+\frac12}}{\bar\rho_R^{i-\frac12}+\bar\rho_L^{i+\frac12}} \int_{-\frac{2\Delta t}{\Delta x}}^0 u\big(w_{a_{i+\frac12}}(\xi;\mathbf{v}_i^n,\mathbf{v}_{i+1}^n)\big)\, dm^-_{i+\frac12}, \tag{3.15}$$

where we have set

$$\bar\rho_L^{i+\frac12} = \bar\rho_L(\mathbf{v}_i^n,\mathbf{v}_{i+1}^n;a_{i+\frac12}) \quad \text{and} \quad \bar\rho_R^{i+\frac12} = \bar\rho_R(\mathbf{v}_i^n,\mathbf{v}_{i+1}^n;a_{i+\frac12}).$$

The measures $dm^\pm_{i+\frac12}$ are defined by:

$$dm^\pm_{i+\frac12} = \frac{\frac{2\Delta t}{\Delta x}\rho\big(w_{a_{i+\frac12}}(\xi;\mathbf{v}_i^n,\mathbf{v}_{i+1}^n)\big)}{\frac{2\Delta t}{\Delta x}\int_0^{\frac{2\Delta t}{\Delta x}}\rho\big(w_{a_{i+\frac12}}(\pm\xi;\mathbf{v}_i^n,\mathbf{v}_{i+1}^n)\big)\, d\xi}\, d\xi.$$

Since the condition (3.12) is satisfied by a the intermediate densities are positive, and then we have $\bar\rho_R^{i-\frac12} > 0$ and $\bar\rho_L^{i+\frac12} > 0$. The measures $dm^\pm_{i+\frac12}$ thus define probability measures. This property satisfied by $dm^\pm_{i+\frac12}$ turns out to be crucial in the sequel to apply the Jensen inequality useful to establish the entropy inequalities.

Now, arguing on the basis of the structure of the Riemann solution, $u\big(w_a(\xi;\mathbf{v}_L,\mathbf{v}_R)\big)\big)$ consists of three distinct values: u_L, u_R and $(u_L+u_R)/2$. As a consequence, we have $u\big(w_a(\xi;\mathbf{v}_L,\mathbf{v}_R)\big)\big) \le \max(u_L,u_R)$. We immediately deduce from (3.15) the expected discrete maximum principle.

Concerning the entropy inequalities, we deduce by the convexity of an otherwise arbitrarily chosen but fixed function S, by the well-known Jensen inequality and from (3.15) the following inequality:

$$S(u_i^{n+1}) \le \frac{\bar\rho_R^{i-\frac12}}{\bar\rho_R^{i-\frac12}+\bar\rho_L^{i+\frac12}} \int_0^{\frac{2\Delta t}{\Delta x}} S\Big(u\big(w_{a_{i-\frac12}}(\xi;\mathbf{v}_{i-1}^n,\mathbf{v}_i^n)\big)\Big)\, dm^+_{i-\frac12} + \frac{\bar\rho_L^{i+\frac12}}{\bar\rho_R^{i-\frac12}+\bar\rho_L^{i+\frac12}} \int_{-\frac{2\Delta t}{\Delta x}}^0 S\Big(u\big(w_{a_{i+\frac12}}(\xi;\mathbf{v}_i^n,\mathbf{v}_{i+1}^n)\big)\Big)\, dm^-_{i+\frac12},$$

which is the desired entropy inequality. The proof is thus complete. ∎

Now, we consider the discrete TVD property of the velocity when establishing the following result:

Theorem 3.4. *Assume that the relaxation parameter a satisfies the condition (3.12). Assume also the validity of the CFL-like condition (3.2). Then, the velocity data are TVD, i.e.,*

$$\mathrm{TV}(\mathbf{u}^n) \le \mathrm{TV}(\mathbf{u}^0)$$

holds for all $n \in \mathbb{N}$.

Proof. In order to establish the TVD property of the velocity data, we propose to write the update formula (3.15) for the variable u in the incremental form (see Godlewski and Raviart [16], or Bouchut [6]).

To do so, let us introduce several pieces of notation. First, from Proposition 3.2, we recall that we have

$$u\big(w_a(\frac{x}{\Delta t};\mathbf{v}_i^n,\mathbf{v}_{i+1}^n)\big)=\begin{cases} u_i & \text{if } x<\mu_1^{i+\frac12},\\ \dfrac{u_i+u_{i+1}}{2} & \text{if } \mu_1^{i+\frac12}<x<\mu_3^{i+\frac12},\\ u_{i+1} & \text{if } x>\mu_3^{i+\frac12},\end{cases}$$

where we have set

$$\mu_1^{i+\frac12}=u_i^n-\frac{a}{\rho_i^n},\qquad \mu_3^{i+\frac12}=u_{i+1}^n-\frac{a}{\rho_{i+1}^n}.$$

Let us recall that $\mu_1^{i+\frac12}<\mu_3^{i+\frac12}$ under the condition (3.12). Next, we set

$$L_1^{i+\frac12}=\max\left(0,\mu_1^{i+\frac12}\right),\qquad l_1^{i+\frac12}=\min\left(0,\mu_1^{i+\frac12}\right),$$
$$L_3^{i+\frac12}=\max\left(0,\mu_3^{i+\frac12}\right),\qquad l_3^{i+\frac12}=\min\left(0,\mu_3^{i+\frac12}\right),$$

to obtain, under the CFL condition (3.2), the formula

$$\begin{aligned} u_i^{n+1}=&\frac{\bar\rho_R^{i-\frac12}}{\bar\rho_R^{i-\frac12}+\bar\rho_L^{i+\frac12}}\times\\ &\left(u_{i-1}^n\int_0^{L_1^{i-\frac12}}dm^+_{i-\frac12}+\frac{u_{i-1}^n+u_i^n}{2}\int_{L_1^{i-\frac12}}^{L_3^{i-\frac12}}dm^+_{i-\frac12}+u_i^n\int_{L_3^{i-\frac12}}\frac{\Delta x}{2\Delta t}dm^+_{i-\frac12}\right)\\ &+\frac{\bar\rho_L^{i+\frac12}}{\bar\rho_R^{i-\frac12}+\bar\rho_L^{i+\frac12}}\times\\ &\left(u_i^n\int_{-\frac{\Delta x}{2\Delta t}}^{l_1^{i+\frac12}}dm^-_{i+\frac12}+\frac{u_i^n+u_{i+1}^n}{2}\int_{l_1^{i+\frac12}}^{l_3^{i+\frac12}}dm^-_{i+\frac12}+u_{i+1}^n\int_{l_3^{i+\frac12}}^{0}dm^-_{i+\frac12}\right).\end{aligned}$$

Since $dm^+_{i+\frac12}$ and $dm^-_{i+\frac12}$ define probability measures on the intervals $(0,\,\frac{\Delta x}{2\Delta t})$ and $(-\frac{\Delta x}{2\Delta t},\,0)$, respectively, we immediately deduce the following incremental coefficients:

$$\begin{aligned} u_i^{n+1}&=C^n_{i+\frac12}u^n_{i+1}+(1-C^n_{i+\frac12}-D^n_{i-\frac12})u_i^n+D^n_{i-\frac12}u^n_{i-1},\\ C^n_{i+\frac12}&=\frac{\bar\rho_L^{i+\frac12}}{\bar\rho_R^{i-\frac12}+\bar\rho_L^{i+\frac12}}\left(\frac12\int_{l_1^{i+\frac12}}^{l_3^{i+\frac12}}dm^-_{i+\frac12}+\int_{l_3^{i+\frac12}}^{0}dm^-_{i+\frac12}\right),\\ D^n_{i-\frac12}&=\frac{\bar\rho_R^{i-\frac12}}{\bar\rho_R^{i-\frac12}+\bar\rho_L^{i+\frac12}}\left(\int_0^{L_1^{i-\frac12}}dm^+_{i-\frac12}+\frac12\int_{L_1^{i-\frac12}}^{L_3^{i-\frac12}}dm^+_{i-\frac12}\right).\end{aligned}$$

A straightforward computation yields that $C^n_{i+\frac12}\geq 0$, $D^n_{i+\frac12}\geq 0$ and $1-C_{i+\frac12{}^n}-D^n_{i-\frac12}\geq 0$ hold for all $i\in\mathbb{Z}$. The proof will be complete as soon as we establish, for all $i\in\mathbb{Z}$, the

relation

$$C^n_{i+\frac{1}{2}} + D^n_{i+\frac{1}{2}} \leq 1,$$

see [16]. Depending on the sign of $\mu_1^{i+\frac{1}{2}}$ and $\mu_3^{i+\frac{1}{2}}$, three cases must be distinguished.

First, let us assume that $\mu_1^{i+\frac{1}{2}} < \mu_3^{i+\frac{1}{2}} < 0$ in order to obtain

$$L_1^{i+\frac{1}{2}} = L_3^{i+\frac{1}{2}} = 0, \quad l_1^{i+\frac{1}{2}} = \mu_1^{i+\frac{1}{2}}, \quad \text{and} \quad l_3^{i+\frac{1}{2}} = \mu_3^{i+\frac{1}{2}}.$$

As a consequence, we have $D^n_{i+\frac{1}{2}} = 0$ and then $C^n_{i+\frac{1}{2}} + D^n_{i+\frac{1}{2}} = C^n_{i+\frac{1}{2}} \leq 1$. Similarly, if we consider $0 < \mu_1^{i+\frac{1}{2}} < \mu_3^{i+\frac{1}{2}}$, we have $C^n_{i+\frac{1}{2}} = 0$ and then $C^n_{i+\frac{1}{2}} + D^n_{i+\frac{1}{2}} = D^n_{i+\frac{1}{2}} \leq 1$. Finally, assume that $\mu_1^{i+\frac{1}{2}} < 0 < \mu_3^{i+\frac{1}{2}}$ to obtain

$$\begin{aligned} C^n_{i+\frac{1}{2}} + D^n_{i+\frac{1}{2}} \;=\; & \frac{1}{\bar\rho_R^{i-\frac{1}{2}} + \bar\rho_L^{i+\frac{1}{2}}} \, \frac{\Delta t}{\Delta x} \int_{\mu_1^{i+\frac{1}{2}}}^{0} \rho\big(w_{a_{i+\frac{1}{2}}}(\xi; \mathbf{v}_i^n, \mathbf{v}_{i+1}^n)\big) \, d\xi \\ & + \frac{1}{\bar\rho_R^{i+\frac{1}{2}} + \bar\rho_L^{i+1+\frac{1}{2}}} \, \frac{\Delta t}{\Delta x} \int_{0}^{\mu_3^{i+\frac{1}{2}}} \rho\big(w_{a_{i+\frac{1}{2}}}(\xi; \mathbf{v}_i^n, \mathbf{v}_{i+1}^n)\big) \, d\xi. \end{aligned}$$

From the identities (3.4) and (3.5), we deduce

$$\begin{aligned} & \frac{\Delta t}{\Delta x} \int_{\mu_1^{i+\frac{1}{2}}}^{0} \rho\big(w_{a_{i+\frac{1}{2}}}(\xi; \mathbf{v}_i^n, \mathbf{v}_{i+1}^n)\big) \, d\xi \leq \frac{\bar\rho_L^{i+\frac{1}{2}}}{2}, \\ & \frac{\Delta t}{\Delta x} \int_{0}^{\mu_3^{i+\frac{1}{2}}} \rho\big(w_{a_{i+\frac{1}{2}}}(\xi; \mathbf{v}_i^n, \mathbf{v}_{i+1}^n)\big) \, d\xi \leq \frac{\bar\rho_R^{i+\frac{1}{2}}}{2}. \end{aligned}$$

We immediately obtain the required inequality $C^n_{i+\frac{1}{2}} + D^n_{i+\frac{1}{2}} \leq 1$. The proof is thus complete. ∎

C. About the approximation of the vacuum

From the works of Bouchut [6], Bouchut and James [8] and Chen and Liu [11], we know that we have to deal with the vacuum problem. Two distinct numerical difficulties must be distinguished in the case of vacuum. First, as soon as the density vanishes, the numerical flux function $\mathcal{F}^n_{i+\frac{1}{2}}$ defined by (3.8) cannot be evaluated since we need to divide by ρ. The second difficulty which arises is related to the computation of a reasonable time step size since we have $\Delta t = O(\Delta x \min(\rho))$. As a consequence, Δt goes to zero as the density vanishes.

In [4], a vacuum correction is proposed. This correction is based on an additional transport equation for the relaxation parameter a. Such an approach allows to consider a variable relaxation parameter, imposing a bound on the ratio a/ρ, *i.e.*, $a = c\rho$ where $c > 0$ is a constant.

In the present work, we establish that no correction is needed by the scheme (3.7)-(3.8) in order to approximate vacuum solutions provided that the following assumption is satisfied: *the initial density is positive*. Let us note that this assumption must also be imposed in order to apply the correction proposed by Bouchut [4].

First, we remark that the updated density ρ_i^{n+1} obtained by the relaxation scheme (3.7)-(3.8) is positive for all $i \in \mathbb{Z}$ as long as $\rho_i^n > 0$ for all $i \in \mathbb{Z}$. Indeed, under

the stability condition (3.12), we have $\rho\big(w_{a_{i+\frac{1}{2}}}(\xi;\mathbf{v}_i^n,\mathbf{v}_{i+1}^n)\big) > 0$ for all $\xi \in \mathbb{R}$ (see Proposition 3.2). Since $\rho_i^{n+1} = (\bar{\rho}_R^{i-\frac{1}{2}} + \bar{\rho}_L^{i+\frac{1}{2}})/2$ where $\bar{\rho}_{L,R}^{i+\frac{1}{2}} = \bar{\rho}_{L,R}(\mathbf{v}_i^n,\mathbf{v}_{i+1}^n;a_{i+\frac{1}{2}})$ is defined by (3.4)-(3.5), we immediately obtain the positivity of the updated density.

Now, the ability of the relaxation scheme (3.7)-(3.8) to approximate vacuum solutions is ensured if we establish that the time increment Δt does not tend to zero as the density goes to zero. In order to assess this issue, we give the following result.

Lemma 3.5. *Let $\epsilon > 0$ and $C > \max(0, u_R - u_L)$ be fixed. Assume that the relaxation parameter a satisfies (3.12). If $u_L \geq u_R$ we have, for all $\xi \in \mathbb{R}$:*

$$\rho\big(w_a(\xi;\mathbf{v}_L,\mathbf{v}_R)\big) \geq \min(\rho_L,\rho_R). \tag{3.16}$$

If $u_L < u_R$, let us assume that

$$0 < a < \min\left(\epsilon, \frac{1}{2}\min(\rho_L,\rho_R)(C + u_L - u_R)\right). \tag{3.17}$$

Then, the following inequality holds for all $\xi \in \mathbb{R}$:

$$\rho\big(w_a(\xi;\mathbf{v}_L,\mathbf{v}_R)\big) \geq \frac{2a}{C} > 0. \tag{3.18}$$

Let us note that the restrictive condition (3.17) is somewhat unusual since it requires a to be small enough while the usual stability condition requires a to be large enough (see the condition (3.12) and also [10, 20, 24]). In fact, as long as $u_L < u_R$ holds, the restriction (3.12) imposes that $a > 0$. Then, the stability condition (3.12) holds for all $a > 0$ such that (3.17) is satisfied.

In the above result, we establish that the intermediate densities decrease as long as $u_L < u_R$. Under the restrictive condition (3.17), the density decreases proportionally to the relaxation parameter a and stays positive. As an immediate consequence, as long as $u_L < u_R$, the eigenvalues are bounded as follows:

$$\begin{aligned}\max(|\mu_1|,|\mu_2|,|\mu_3|) &= \max\left(\left|\frac{u_L+u_R}{2} - \frac{a}{\rho_L^\star}\right|, \left|\frac{u_L+u_R}{2}\right|, \left|\frac{u_L+u_R}{2} + \frac{a}{\rho_R^\star}\right|\right)\\ &\leq \left|\frac{u_L+u_R}{2}\right| + \frac{C}{2},\end{aligned}$$

where the intermediate states are defined in Proposition 3.2. In other words, the eigenvalues are bounded as the density tends to zero. By employing the CFL-like condition (3.2), the time increment Δt does not tend to zero as the density decreases to zero.

In the numerical experiments, we will impose $C > \mathrm{TV}(u^0)$, where u^0 defines the initial velocity. Indeed, considering the TVD property of the velocity, we have $C > \mathrm{TV}(u^0) > \max(0, u_{i+1}^n - u_i^n)$ for all $i \in \mathbb{Z}$ and $n \in \mathbb{N}$.

We conclude the present section with the proof of Lemma 3.5.

Proof. In the Riemann solution, $\rho\big(w_a(\xi;\mathbf{v}_L,\mathbf{v}_R)\big)$ is made up of

$$\rho_L, \quad \rho_R, \quad \frac{1}{\dfrac{1}{\rho_L} + \dfrac{u_R-u_L}{2a}}, \quad \frac{1}{\dfrac{1}{\rho_R} + \dfrac{u_R-u_L}{2a}}.$$

First assume that $u_L < u_R$ to obtain, under the condition (3.17), after a straightforward computation the expected estimation (3.18). Similarly, (3.16) is a direct consequence of the structure of the Riemann solution with $u_L > u_R$. ∎

IV. NUMERICAL RESULTS

In this section, we perform several numerical tests using the relaxation scheme (3.7)-(3.8) we have investigated as well as a straightforward second-order MUSCL-type extension; the reader is refered to Godlewski and Raviart [16] or LeVeque [19] for further details concerning this type of high-resolution schemes. The second order extension is performed using a linear reconstruction on the characteristic variables (ρ, u). The classical *minmod* function is considered for the slope limitation (see [16, 19]).

First, we propose 1-D tests devoted to approximate vacuum solutions and a delta-shock solution. These approximate solutions are systematically compared with the numerical solutions obtained by the first- and second-order kinetic schemes proposed by Bouchut in [9], respectively. In all the corresponding numerical tests, we use a uniform 200 points mesh and the CFL number is fixed at 0.5. Finally, we consider a twodimensional test case employing a 2-D extension of the developed relaxation scheme.

In the first test, we consider the following initial data:

$$\rho^0(x) = 0.5, \qquad u^0(x) = \begin{cases} -0.5 & \text{if } x < -0.5, \\ 0.4 & \text{if } -0.5 < x < 0, \\ 0.4 - x & \text{if } 0 < x < 0.8, \\ -0.4 & \text{if } x > 0.8. \end{cases}$$

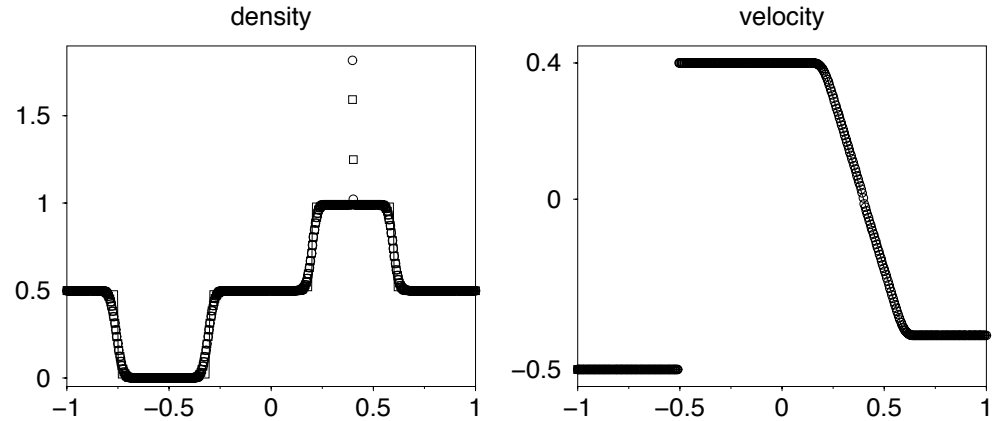

FIG. 1. Comparison of results of the first experiment showing the exact solution (lines) together with the numerical results obtained by the first-order kinetic scheme (boxes) and the proposed relaxation method (circles).

The approximate solutions obtained using the first-order kinetic and relaxation scheme, respectively, are displayed in Figure 1 and are compared with the exact solution. We

obtain a fairly good agreement except for a spike within the density due to some inconsistency at the sonic point that was already noticed in [6].

In the second numerical test, see Figure 2, we focus our attention on the vacuum problem. Therefore, we consider the initial data

$$\rho^0(x) = 0.5, \qquad u^0(x) = \begin{cases} -0.5 & \text{if } x < 0, \\ 0.4 & \text{if } x > 0. \end{cases}$$

The exact solution at time $t = 0.5$ is

$$\rho^0(x) = \begin{cases} 0.5 & \text{if } x < -0.25, \\ 0 & \text{if } -0.25 < x < 0.2, \\ 0.5 & \text{if } x > 0.2, \end{cases}$$

$$u^0(x) = \begin{cases} -0.5 & \text{if } x < -0.25, \\ undefined & \text{if } -0.25 < x < 0.2, \\ 0.4 & \text{if } x > 0.2. \end{cases}$$

For both first-order schemes, the vacuum approximation at time $t = 0.5$ is obtained after 100 iterations. This illustrates Lemma 3.5, since even if the density is very close to zero, the number of time iterations remains bounded. In Figure 3 we display the minimal density obtained in the vacuum approximation when using both first-order schemes. Let us note that that the minimal density obtained with the kinetic scheme is of the order of magnitude 10^{-15} while the minimal density computed by the relaxation scheme is close to 10^{-323}.

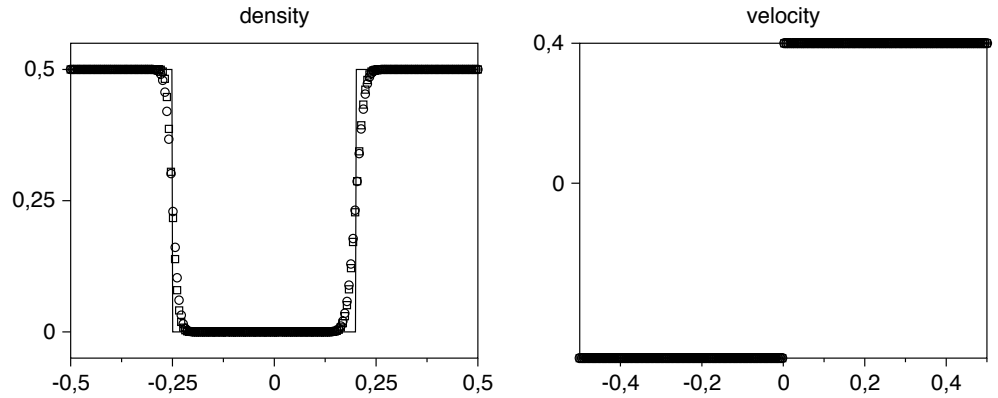

FIG. 2. Comparison of first-order results of the vacuum experiment, showing analogously to the first figure the exact solution (lines) together with the numerical results obtained by the kinetic scheme (boxes) and the proposed relaxation scheme (circles).

We now employ as indicated the second-order MUSCL-type relaxation scheme, comparing it with the second-order kinetic scheme from [9]. The second-order approximate solution is displayed in Figure 4. As expected, we observe the effect of smaller dissipation compared to the first-order schemes when approximating the discontinuities. In Figure 5, the minimal density and the L^1-error for the schemes of interest are displayed. Let us note that the L^1-error graphs involve straight lines with the slopes 0.5 and 1 for

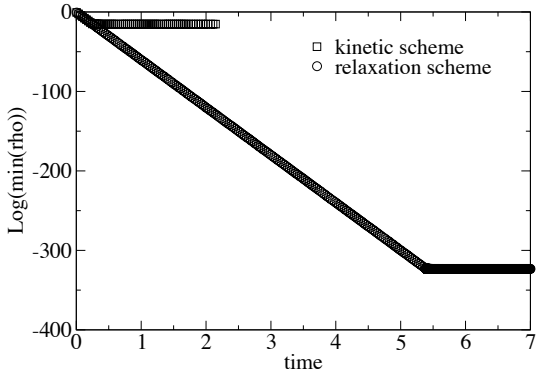

FIG. 3. Logarithmic minimal density versus time in the vacuum experiment, showing the numerical results obtained by the kinetic scheme (boxes) and the relaxation scheme (circles).

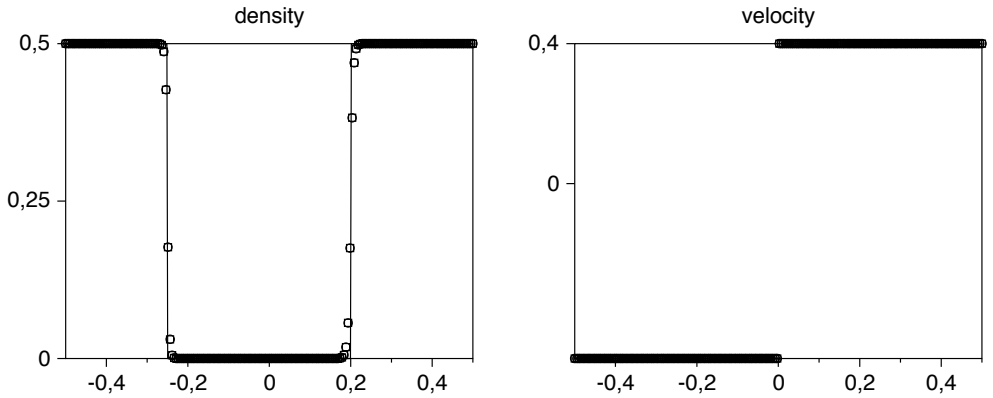

FIG. 4. Comparison of second-order results of the vacuum experiment, showing the exact solution (lines) together with the numerical results obtained by the kinetic scheme (boxes) and the relaxation scheme (circles).

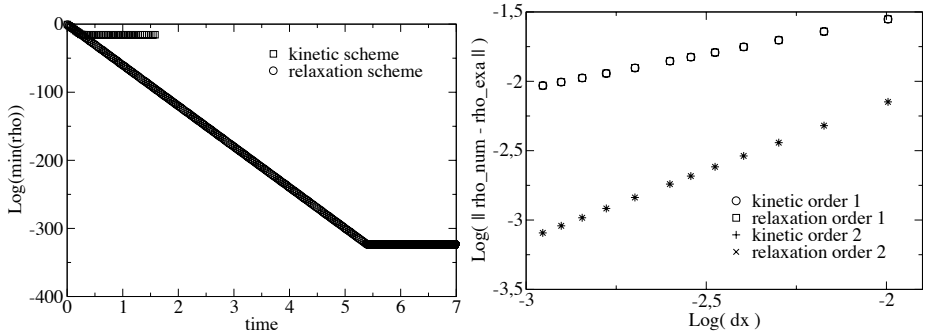

FIG. 5. Logarithmic minimal density obtained using the discussed second-order schemes versus time and logarithmic L^1-error versus logarithmic space increment Δx in the vacuum experiment.

the first-order and second-order schemes, respectively: this coincides with the expected convergence rates (given by $\sqrt{\Delta x}$) when approximating discontinuous solutions.

The last 1-D numerical experiment is devoted to the delta-shock. In Figure 6, we display the numerical result obtained at the time $t = 0.5$ for the following initial data:

$$\rho^0(x) = \begin{cases} 1 & \text{if } x < -0, \\ 0.25 & \text{if } x > 0, \end{cases} \qquad u^0(x) = \begin{cases} 1 & \text{if } x < 0, \\ 0 & \text{if } x > 0. \end{cases}$$

A delta-shock is immediately developed and the shock speed is 2/3. Both the numerical schemes are able of capturing the delta-shock with the correct propagation speed.

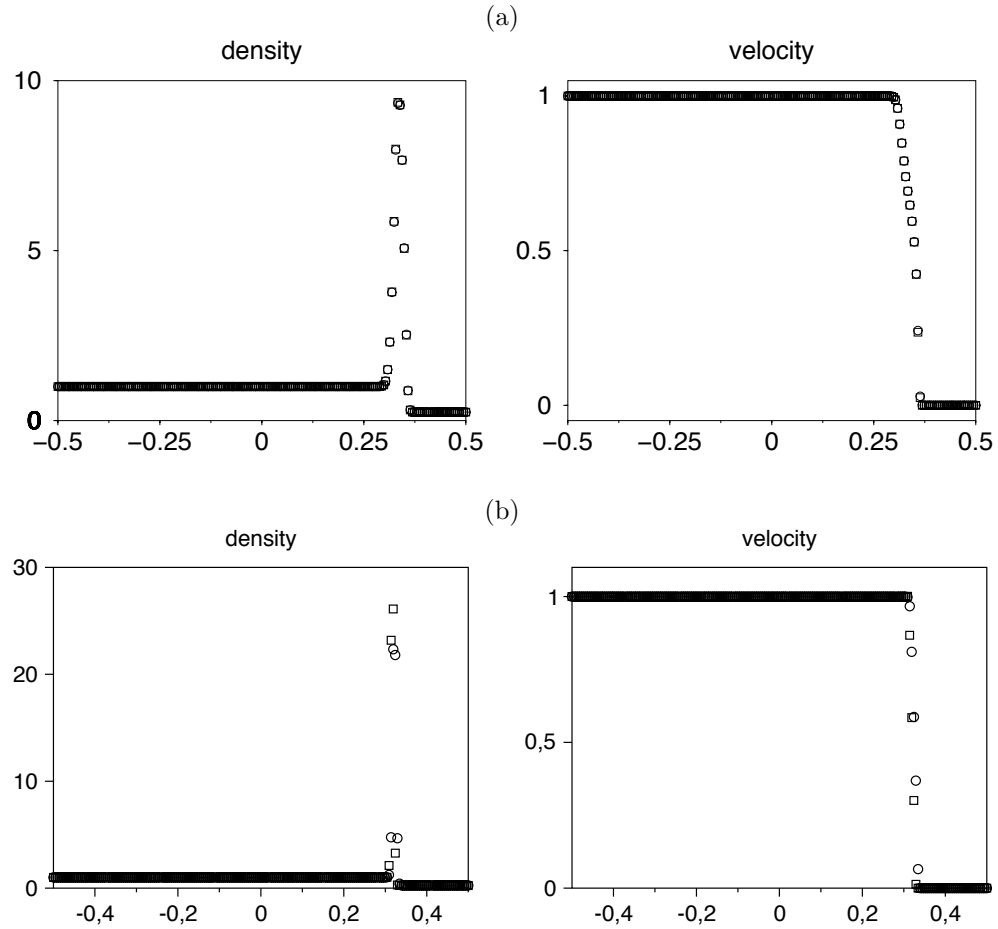

FIG. 6. Comparison of (a) first-order and (b) second-order numerical approximations for the delta-shock experiment, showing the numerical results obtained by the corresponding kinetic schemes (boxes) and the relaxation schemes (circles), respectively.

The last numerical experiment we have considered in the present paper is devoted to a bidimentional simulation. From (1.1), we recall that the 2-D pressureless gas dynamics equations read as follows:

$$\begin{cases} \partial_t \rho + \partial_x \rho u + \partial_y \rho v = 0, & (x, y) \in \mathbb{R}^2,\ t > 0, \\ \partial_t \rho u + \partial_x \rho u^2 + \partial_y \rho uv = 0, \\ \partial_t \rho v + \partial_x \rho uv + \partial_y \rho v^2 = 0. \end{cases} \tag{4.1}$$

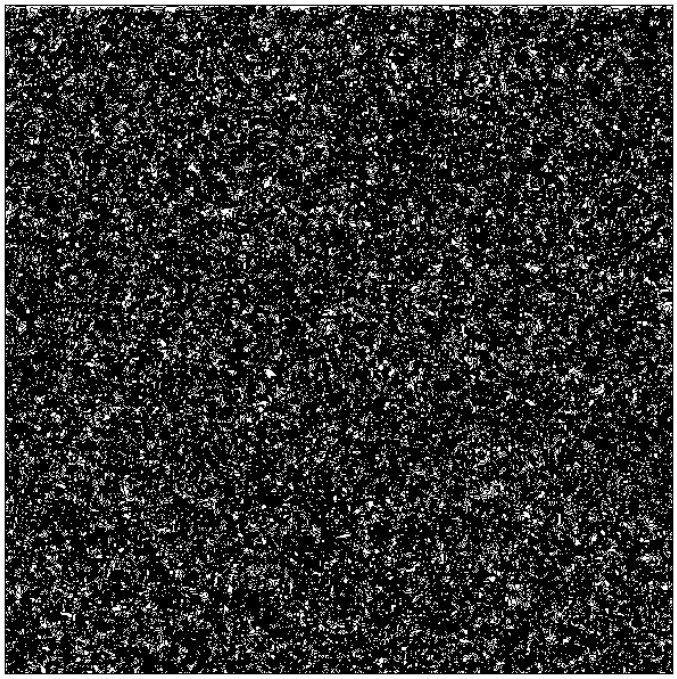

FIG. 7. Initial density distribution.

We adopt a standard 2-D extension procedure and we refer the reader to Godlewski and Raviart [16] or LeVeque [19] for further details. We briefly recall that the variable $\mathbf{u} = (\rho, \rho u, \rho v)^T$ is updated as follows:

$$\mathbf{u}_i^{n+1} = \mathbf{u}_i^n - \frac{\Delta t}{\mathcal{A}_i} \sum_{i \in \vartheta(i)} \phi_{ij},$$

where $\mathcal{A}_i$ is the area of the corresponding cell and where $\vartheta(i)$ denotes the set of neighboring cells for the cell i. The numerical flux ϕ_{ij} is computed from the approximate solution of the Riemann problem given at the cell interface:

$$\phi_{ij} = \phi(\mathbf{n}_{ij}, \mathbf{u}_i, \mathbf{u}_j),$$

where $\mathbf{n}_{ij}$ is the normal to the cell interface between the cells i and j which points from cell i to cell j.

The physical model considered here is derived from large scale structure simulations; for instance, see the work of Vergassola, Dubrulle, Frisch and Noullez [23] or the work of Zeldovich [26]. In fact, the system (4.1) coincides with the Zeldovich approximation in the absence of the expansion of the universe and the gravitational potential. We consider well-prepared initial data where ρ^0 is a Gaussian field, see Figure 7, and where the initial velocity vector is the solution of

$$\begin{cases} u = -\partial_x \phi, \\ v = -\partial_y \phi, \\ \Delta \phi = 4\Pi G(\rho - \rho_b) \qquad \text{over } \Omega, \end{cases}$$

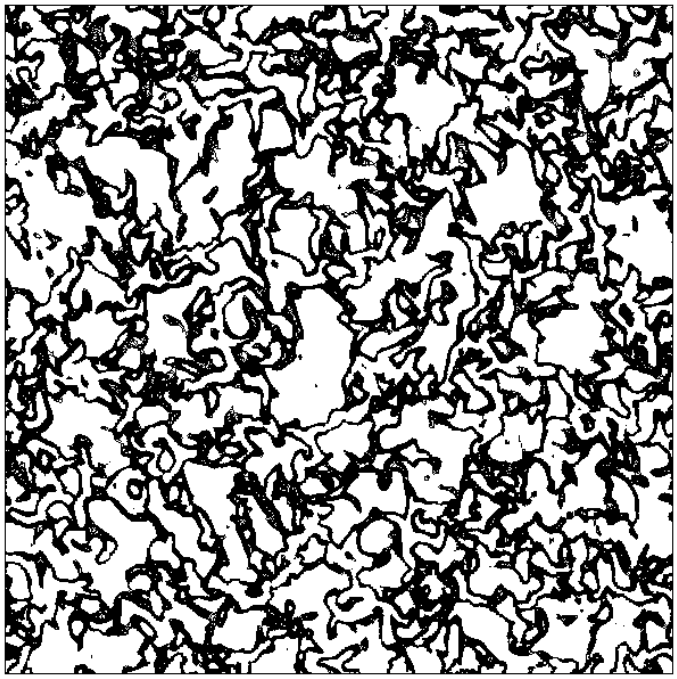

FIG. 8. A typical intermediate state obtained by the 2-D version of our relaxation method. We clearly observe the arising filament structure within the density distribution.

with $G > 0$ a constant and $\rho_b = \int_\Omega \rho \, dxdy$. All boundary conditions are assumed to be periodic.

In Figures 8 and 9, we observe the evolution of the large-scale structures. The numerical results are analogous to results obtained in cosmological applications, see for instance [23]. However, in the present work, no cosmological interpretations are proposed since the expansion and gravitational potential have been omitted.

The second author would like to thank the Deutsche Forschungsgemeinschaft (DFG) for supporting his research by grant No. BR 2245/1-1.

REFERENCES

1. R.K. Agarwal and D.W. Halt, "Frontiers of Computational Fluid Dynamics", David A. Caughey and Mohamed M. Hafez (Eds.), 1994, 155–163.

2. R. Baraille, G. Bourdin, F. Dubois and A.Y. LeRoux (1992), "Une version à pas fractionnaires du schema de Godunov pour l'hydrodynamique", *C.R. Acad. Sci. Paris*, t. 314, Série 1, 147–152.

3. M. Baudin, C. Berthon, F. Coquel, R. Masson and Q. H. Tran (2005), "A relaxation method for two-phase flow models with hydrodynamic closure law", *Num. Math.*, **99**, No 3, 411–440.

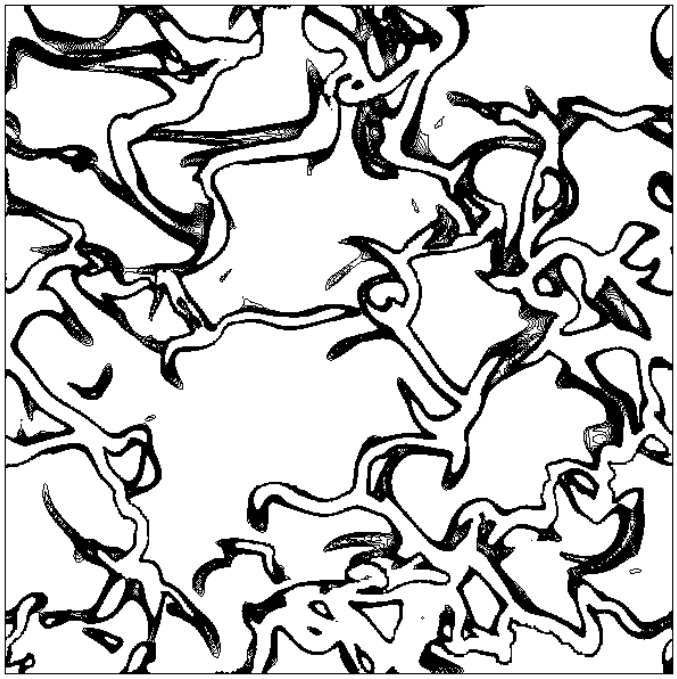

FIG. 9. A typical state obtained by long term computations. The distinguished filament structure already observable in Figure 8 has formed more clearly.

4. F. Bouchut (2004), "Nonlinear stability of finite volume methods for hyperbolic conservation laws, and well-balanced schemes for sources", Frontiers in Mathematics series, Birkhuser.
5. F. Bouchut (2003), "Entropy satisfying flux vector splittings and kinetic BGK models", *Numer. Math.*, **94**, No 4, 623–672.
6. F. Bouchut (1994), "On zero pressure gas dynamics", *Series on Advances in Mathematics for Applied Sciences*, World Scientific, **22**, 171–190.
7. F. Bouchut and G. Bonnaud (1996), "Numerical Simulation of Relativistic Plasmas in Hydrodynamic Regime", *ZAMM*, **76**, 287–290.
8. F. Bouchut and F. James (1999), "Duality solutions for pressureless gases, monotone scalar conservation laws, and uniqueness", *Comm. Partial Diff. Eq.*, **24**, 2173–2189.
9. F. Bouchut, S. Jin and X. Li (2003), "Numerical approximations of pressureless and isothermal gas dynamics", *SIAM J. Num. Anal.*, **41**, 135–158.
10. G.Q. Chen, C.D. Levermore and T.P. Liu (1995), "Hyperbolic Conservation Laws with Stiff Relaxation Terms and Entropy", *Comm. Pure Appl. Math.*, **47**, 787–830.
11. G.-Q. Chen and H. Liu (2003), "Formation of δ-Shocks and Vacuum States in the Vanishing Pressure Limit of Solutions to the Euler Equations for Isentropic Fluids" *SIAM J. Math. Anal.*, **34**, No 4, 925–938.
12. F. Coquel, E. Godlewski, A. In, B. Perthame and P. Rascle (2002), "Some new Godunov and relaxation methods for two phase flows", *Proceedings of an International conference on Godunov methods: Theory and Applications*, Kluwer Academic/Plenum Publishers.

13. F. Coquel and B. Perthame (1998), "Relaxation of Energy and Approximate Riemann Solvers for General Pressure Laws in Fluid Dynamics", *SIAM J. Numer. Anal.*, **35**, 6, 2223–2249.

14. B. Einfeldt, C.-D. Munz, P.L. Roe and B. Sjögreen (1991), "On Godunov-type methods near low densities", *J. Comput. Phys.*, **92**, No 2, 273–295.

15. W. E, Yu. G. Rykov and Ya. G. Sinai, "Generalized variation principles, global weak solutions and behaviour with random initial data for systems of conservation laws arising in adhesion particle dynamics", *Commun. Math. Phys.*, **177** (1996), pp. 349-380.

16. E. Godlewsky and P.A. Raviart, *Numerical Approximation of Hyperbolic System of Conservation Laws*, Applied Mathematical Sciences, **118**, Springer, New-York, 1996.

17. A. Harten, P.D. Lax and B. van Leer (1983), "On Upstream Differencing and Godunov-Type Schemes for Hyperbolic Conservation Laws", *SIAM Review*, **25**, 35–61.

18. S. Jin and Z. Xin (1995), "The Relaxation Scheme for Systems of Conservation Laws in Arbitrary Space Dimension", *Comm. Pure Appl. Math.*, **45**, 235–276.

19. R.J. LeVeque, *Finite volume methods for hyperbolic problems*, Cambridge University Press, Cambridge, 2002.

20. T.P. Liu (1987), "Hyperbolic conservation laws with relaxation", *Comm. Math. Phys.*, **108**, 153–175.

21. W. Sheng and T. Zhang (1999), "The Riemann Problem for the Transportation Equations in Gas Dynamics", *Mem. Amer. Math. Soc.*, **137**.

22. I. Suliciu (1998), "Energy estimates in rate-type thermo-viscoplasticity", *Int. J. Plast.*, **14**, 227–244.

23. M. Vergassola, B. Dubrulle, U. Frisch and A. Noullez (1994), "Burgers equations, Devil's staircases and the mass distribution for large scale structures", *Astron. Astrophys*, **289**, 325–356.

24. J. Whitham (1974), *Linear and Nonlinear Waves*, Wiley, New-York.

25. Li Yinfan and Cao Yiming (1985), "Large particle difference method with second order accuracy in gas dynamics", *Scientic Sinica (A)*, **28**, 1024–1035.

26. Ya. B. Zeldovich (1970), "Gravitational instability: An approximate theory for large density perturbations", *Astron. Astrophys*, **5**, 84–89.